Geomorphology xxx (2011) xxx–xxx

Contents lists available at SciVerse ScienceDirect

Geomorphology

journal homepage: www.elsevier.com/locate/geomorph

Erosion rates and erosion patterns of Neogene to Quaternary stratovolcanoes in the Western Cordillera of the Central Andes: An SRTM DEM based analysis

D. Karátson [a,b,*], T. Telbisz [a], G. Wörner [b]

[a] Department of Physical Geography, Eötvös University, Pázmány s. 1/c, H-1117 Budapest, Hungary
[b] Geoscience Center, Georg-August University Göttingen, Goldschmidtsrasse 1, 37077 Göttingen, Germany

ARTICLE INFO

Article history:
Received 15 October 2010
Received in revised form 6 October 2011
Accepted 8 October 2011
Available online xxxx

Keywords:
Volcanic geomorphology
DEM-morphometry
Stratovolcano erosion
Central Andes
Climate

ABSTRACT

Erosion patterns and rates of 33 stratovolcanoes in the arid to hyperarid Central Andean Volcanic Zone (14°S to 27°S) have been constrained by morphometric modelling. All selected volcanoes belong to the short-lived, symmetrical, circular andesitic stratocone type, with ages spanning 14 Ma to recent. Starting from the initial, youthful volcano morphology of this type, represented in our study by Parinacota volcano, and comparing reconstructed volumes of progressively eroded volcanoes, such a time span allows us to infer long-term erosion rates. Typical erosion rates of <10 to 20 m/Ma have been obtained for the Altiplano–Puna Plateau. Lowest erosion rates typify the hyperarid Puna plateau (7–9 m/Ma), while somewhat higher values (13–22 m/Ma) are recorded for volcanoes in the more humid South Peru, suggesting climatic control on differences in erosion rates. By contrast, much higher short-term erosion rates of 112 to 66 m/Ma, decreasing with age, are found for young (Late Quaternary) volcanoes, which indicates that juvenile volcanoes erode more rapidly due to their unconsolidated cover and steeper slopes; surface denudation slows down to approximately one tenth of this after a few Ma. An inverse correlation is observed between the degree of denudation (defined as volume removed by erosion/original volume) and edifice height from base to top after erosion. This relationship is independent of climate and original edifice elevation. The degree of denudation vs. volcano age provides a rough morphometric tool to constrain the time elapsed since the extinction of volcanic activity. This method can, however, only be applied to the volcanoes of the Altiplano (i.e. under uniform, long-term arid climate) with an uncertainty of ~1 Ma. Finally, an erosional pathway is suggested for volcanoes of the Altiplano–Puna preserving a peculiar "edelweiss" valley pattern related to glaciations. This pattern may have overprinted previous drainages and resulted in a discontinuous height reduction of the degrading stratovolcanoes.

1. Introduction

Neogene to Quaternary volcanoes of the Central Andes comprise a great number of poorly known, hardly accessible edifices, many of which have an altitude well above 5000 m (including the highest volcanoes on Earth, >6500 m in elevation). Detailed research has been concentrated on Quaternary and recently active volcanoes (e.g. Parinacota, Lascar, Ubinas, El Misti, San Pedro–San Pablo, to name a few). However, most of the extinct cones are little studied and no more information is available than the general statement by de Silva and Francis (1991): "On Landsat images of the Central Andes there are well in excess of 1000 topographic features whose distinctive morphologies indicate that they are volcanoes"; (…) "given the slow erosion rates many of these may be as much as 5–10 million years old".

A main reason for the abundance of extremely well preserved volcanic structures in this area, especially in the Altiplano–Puna plateau (Davidson and de Silva, 2000), lies in the fact that arid climates have persisted at least since ~15 Ma (Alpers and Brimhall, 1988; Hartley, 2003; Ehlers and Poulsen, 2009; Garreaud et al., 2010). These unusual climate conditions resulted in extremely low erosion rates and therefore strato- and shield volcanoes as old as 14 Ma can still be easily recognized. Moreover, apart from the generally arid climate, there is a systematic precipitation gradient from S to N along the western Andean orogenic front, from the hyperarid Puna through the arid Altiplano to semi-humid South Peru (Placzek et al., 2006), regardless of smaller-scale climatic fluctuations. There are thus a large number of volcanic structures ranging from old preserved volcanoes to active ones, having different edifice ages, edifice height, basal elevation above sea level, and location with respect to the precipitation gradient. Consequently, this region on Earth provides a unique opportunity to quantify long-term erosion rates of volcanoes under ~15 Ma-long continuously arid climate conditions.

Our study is based on data from the Shuttle Radar Topography Mission (SRTM) which provides a 90 m spatial resolution DEM on most of the Earth's surface (Rabus et al., 2003; Berry et al., 2007; Farr et al., 2007). This resolution is appropriate for quantifying the

* Corresponding author at: Department of Physical Geography, Eötvös University, Pázmány s. 1/c, H-1117 Budapest, Hungary.
E-mail address: dkarat@ludens.elte.hu (D. Karátson).

0169-555X/$ – see front matter © 2011 Elsevier B.V. All rights reserved.
doi:10.1016/j.geomorph.2011.10.010

geomorphology of large stratovolcanoes (Karátson and Timár, 2005; Wright et al., 2006; Kervyn et al., 2008; Grosse et al., 2009; Karátson et al., 2010a). The global ASTER DEM with a 30 m cell size was released more recently (Hayakawa et al., 2008) but has many artefacts and is not more accurate in terms of elevation (e.g. Bolch et al., 2005; Crippen et al., 2007; Huggel et al., 2008; Hirt et al., 2010).

Here, applying a morphometric approach, we investigate the erosion of stratovolcanoes of the Central Andes (Fig. 1). To quantify long-term erosion (1) we have to select volcanoes of different age and different degree of denudation, and for the reliable comparison (2) we need to use uniform initial volcano shapes. However, in the Central Andes, there is a large range of volcano types with different morphologies such as dome complexes, monogenetic centres, shields, complex dome–cone edifices etc. (cf. de Silva and Francis, 1991; Grosse et al., 2009). Yet, a great number of edifices display a simple, regular cone shape, these volcanoes being typically composed of mafic andesites and predominantly constructed by lava flows. They not only stand out by their very regular shape but also by their short (<100–200 ka) life times (see Thouret et al., 2001; Hora et al., 2007 for examples and references). In the Central Andes these mafic andesite volcanoes tend to form in regional clusters of similar age (Wörner et al., 2000). Petrological and volcanological similarities of simple Central Andean stratovolcanoes are also shown by a number of studies (de Silva and Francis, 1991; Davidson and de Silva, 2000; Trumbull et al., 2006). They have a typical range in SiO_2 from 55 to 60%, which corresponds predominantly to andesitic lava flows comprising the edifice. More evolved rocks in this type are rare and of small volume (i.e. dacitic and rhyodacitic domes, dome clusters as well as related pyroclastic

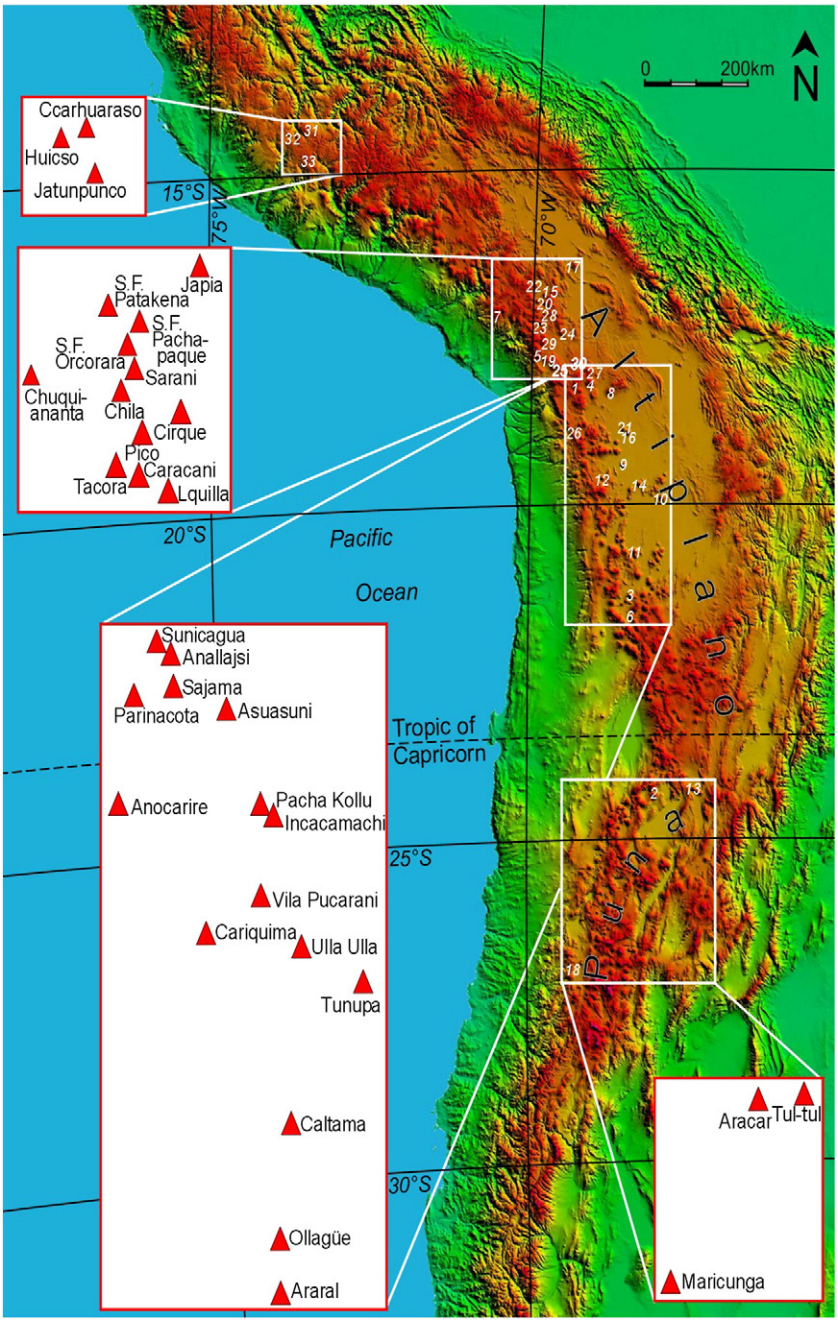

Fig. 1. Location of the volcanoes studied. Numbering is the same as in Table 1. All volcanoes are located at or near the Western Cordillera in three principal geographic settings: (a) volcanoes located in regions with deeply incised valley systems (South Peru, around 15°S, 3 volcanoes), (b) along the westernmost margin of the Altiplano (16° to 23°S, 27 volcanoes) and (c) in the southern Puna region (24° to 28°S) where several tectonic basins and ridges modify the Andean plateau morphology (e.g. Antofalla rift; 3 volcanoes).

Please cite this article as: Karátson, D., et al., Erosion rates and erosion patterns of Neogene to Quaternary stratovolcanoes in the Western Cordillera of the Central Andes: An SRTM DEM based analysis, Geomorphology (2011), doi:10.1016/j.geomorph.2011.10.010

Table 1
Geographical, morphometric, volumetric and chronological data of the studied volcanoes of the Central Andes. Bold data are the degree of denudation and erosion rates. C = Cerro, N = Nevado.

Volcano					Morphometry							Erosion calculation					Dating		
	Name	Lat.	Long.	Country	Summit elevation	Base level	Edifice height (H)	Area	Height/ diameter (H/D)	Reconstructed volume	Present volume	Erosion	Degree of denudation	Degree of denud. error	Surface lowering	Erosion Rate	K/Ar age	"Erosional" age	Diff. from K/Ar
					m a.s.l.	m a.s.l.	m a. base	km^2		km^3	km^3	km^3	%	%	m	m/Ma	Ma	Ma	Ma
1	Parinacota	−18.17	−69.15	Chile	6328	4560	1768	170.6	0.12	40.6	40.6	0	**0**				2.6 ka[a]		
2	C. Aracar (Puna)	−24.29	−67.79	Argentina	6064	4100	1964	192.4	0.13	63.4	61.6	1.8	**2.8**	0.6	9	**93.6**	~0.1[b]	−0.1	−0.2
3	Ollagüe	−21.30	−68.17	Chile/ Bolivia	5851	3800	2051	246.6	0.12	92.3	88.7	3.6	**3.9**	0.9	15	**112.3**	0.13 ± 0.04[1]	0.4	0.2
4	N. Sajama	−18.10	−68.88	Bolivia	6547	4050	2497	496.8	0.10	255.3	237.7	17.6	**6.9**	1.4	35			1.4	
5	Tacora	−17.72	−69.77	Chile	5953	4100	1853	129.9	0.14	57.3	53.1	4.2	**7.3**	1.7	32	**66.1**	0.489 ± 0.015[2]	1.6	1.1
6	C. Araral	−21.60	−68.18	Chile/ Bolivia	5647	3900	1747	109.4	0.15	47.2	43.4	3.8	**8.1**	1.8	35			1.9	
7	N. Chuquiananta	−17.08	−70.47	Peru	5538	4000	1538	364.4	0.07	248.1	219.1	29	**11.7**	2.1	80	**24.6**	3.23 ± 0.5[3]	3.2	0.0
8	C. Asuasuni	−18.23	−68.53	Bolivia	5099	3900	1199	433.2	0.05	138.6	121.4	17.2	**12.4**	2.7	40			3.4	
9	C. Vila Pucarani	−19.32	−68.30	Bolivia	4887	3700	1187	268.4	0.06	89.1	77.4	11.7	**13.2**	2.9	44			3.7	
10	C. Tunupa	−19.83	−67.63	Bolivia	5303	3700	1603	203.3	0.10	84.6	72.7	11.8	**14**	2.7	58			4.0	
11	C. Caltama	−20.65	−68.12	Bolivia	5358	3700	1658	179.7	0.11	88.9	76.4	12.5	**14.1**	2.9	70			4.1	
12	C. Cariquima	−19.53	−68.67	Chile	5366	3820	1546	123.3	0.12	42.7	36	6.7	**15.7**	3.8	54			4.6	
13	C. Tul-tul (Puna)	−24.19	−64.10	Argentina	5262	3800	1462	106.7	0.13	40.1	33.3	6.8	**16.9**	3.2	64	**8.7**	7.3 ± 0.7[4]	5.1	−2.2
14	C. Ulla Ulla	−19.62	−68.03	Bolivia	5036	3720	1316	103.9	0.11	47.1	38.7	8.3	**17.7**	3.3	80			5.4	
15	C. San F. Pachapaque	−16.80	−69.66	Peru	4923	4000	923	105	0.08	41.6	33.3	8.3	**20**	3.5	79			6.2	
16	C. Incacamachi	−18.87	−68.22	Bolivia	4776	3700	1076	169.6	0.07	50.9	38.9	12	**23.5**	5.7	71			7.5	
17	C. Japia	−16.35	−69.15	Peru	4795	3840	955	417.1	0.04	117.3	89.5	27.7	**23.6**	5.1	66	**9.2**	7.2 ± 0.09[5]	7.5	0.3
18	C. Maricunga (Puna)	−27.00	−69.20	Chile	4972	3800	1172	221.8	0.07	100.5	77.5	23	**23.7**	3.8	104	**7.1**	14.6 ± 0.6[6]	7.6	−7.0
19	C. Caracani	−17.75	−69.62	Chile	5175	4100	1075	263.5	0.06	126.1	95	31.1	**24.7**	4.1	118			7.9	
20	C. San F. Orcorara	−16.88	−69.77	Peru	5012	4100	912	119.6	0.07	35.4	26.4	9	**25.3**	6.6	75			8.1	
21	C. Pacha Kollu	−18.80	−68.30	Bolivia	4756	3730	1026	107.9	0.09	37.4	27.7	9.6	**25.8**	5.3	89			8.3	
22	C. San F. Patakena	−16.65	−69.83	Peru	5015	4200	815	103.9	0.07	43.5	31.8	11.7	**26.9**	4.1	113			8.7	
23	C. Chila	−17.22	−69.72	Peru	5157	4230	927	115.9	0.08	38.9	28.3	10.5	**27.1**	7.0	91			8.8	
24	C. Cirque	−17.35	−69.37	Bolivia	5067	4100	967	235.6	0.06	87.2	61.7	25.5	**29.2**	6.0	108			9.6	
25	C. Lquilla (Cosapilla)	−17.85	−69.50	Chile	5322	4200	1122	184.1	0.07	65.2	45.7	19.4	**29.8**	5.8	105			9.8	
26	C. Anocarire	−18.78	−69.23	Chile	4996	4100	896	142.4	0.07	55	38.5	16.5	**30**	5.6	116	**11.1**	10.4 ± 0.7[7]	9.9	−0.5
27	C. Anallajsi	−17.93	−68.90	Bolivia	5549	4200	1349	368.8	0.06	154.5	106.8	47.7	**30.9**	5.8	129			10.2	
28	C. Sarani	−17.15	−69.68	Peru	5072	4250	822	91.7	0.08	33	22.3	10.8	**32.6**	5.7	118			10.8	
29	C. Pico	−17.52	−69.68	Peru	5405	4340	1065	159.8	0.07	76.1	50.6	25.5	**33.5**	5.3	160			11.1	
30	C. Sunicagua	−17.87	−68.98	Bolivia	4999	4230	769	134.1	0.06	44.9	29.2	15.7	**35**	8.5	117			11.7	
31	C. Ccarhuaraso (Peru)	−14.32	−73.78	Peru	5076	4000	1076	616.8	0.04	294.9	172.2	122.6	**41.6**	5.9	199	**21.6**	9.2 ± 0.5[8]	14.1	4.9
32	C. Huicso (Peru)	−14.40	−74.02	Peru	4599	4000	599	157.2	0.04	64.5	37.3	27.1	**42.1**	6.9	172			14.3	
33	C. Jatunpunco (Peru)	−14.73	−73.72	Peru	5143	4400	743	341.6	0.04	131.3	67	64.3	**49**	8.1	188	**13.1**	14.35 ± 0.7[9]	16.8	2.4
	Min				*4599*	*3700*	*599*	*91.7*	*0.04*	*33*	*22.3*	*3.6*	***3.9***	*0.9*	*9*	***7.1***			
	Max				*6547*	*4400*	*2497*	*616.8*	*0.15*	*294.9*	*237.7*	*122.6*	***49.0***	*8.5*	*188*	***112.3***			
	Average				*5215*	*3991*	*1224*	*217.7*	*0.08*	*88.9*	*69.1*	*19.8*	***21.8***	*4.3*	*89*	***36.8***			

1, 2 — Wörner et al. (2000); 3, 5 — Kaneoka and Guevara (1984); 4 — Vandervoort et al. (1995); 6 — McKee et al. (1994); 7 — Charrier et al. (2004); 8, 9 — Bellon and Lefèvre (1977).
[a] Last eruption 2.6 ka ago (Hora et al., 2007).
[b] Possible age based on Bull. Global Volcanism Network report 04/1993 BGVN 18:04.

rocks). Those Andean volcanoes that significantly deviate from the simple stratocone type are also characterized by a larger range in lithologies, and often show much longer life times. Therefore, by restricting the selection to the simple stratocones, we effectively exclude the lithological factors which may influence the overall rates and patterns of erosion.

The selected 33 stratovolcanoes (Table 1) are located from South Peru through Bolivia and Northern Chile to Northwest Argentina in the quadrangle of 14°S, 64°W and 27°S, 74°W. In addition to the single, symmetrical cone shape, the location on a relatively flat basement and no overlap with other volcanic centres has been preferred. Our volcano data base comprises a range from young, almost intact conical forms to older, differently eroded and dissected edifices, whose initially simple cone is still recognizable despite the effects of long-term degradation.

Our selection includes 11 volcanoes that have K/Ar or Ar/Ar ages. The oldest volcano is Mid-Miocene, but the ages are distributed throughout the Pliocene and Quaternary that allows us to draw general conclusions on volcano erosion with time. The majority of the volcanoes have only one single age date, which puts into question the exact timing of extinction, i.e. the starting point of erosion. However, as mentioned, the selected simple stratovolcanoes may have been constructed during relatively short cone-building stages (Davidson and de Silva, 2000). Although erosion and collapse may occur between these stages, the final cone shape is not necessarily influenced: for example, the perfect cone of Parinacota volcano has been completely rebuilt after a collapse event 15–20 ka ago (Hora et al., 2007).

Because erosion time (typically several millions of years) is one or two orders of magnitude longer than volcano life time, and because morphological, structural and possibly lithological similarities between the selected stratocones imply a short building stage similar to Parinacota, even a single radiometric date may provide an approximate starting point for erosion (particularly for older, more eroded edifices).

We emphasize that during volcano life time, erosion concomitant to edifice growth can also be significant. However, overall construction greatly exceeds erosion up to the final stage, i.e. a youthful cone shape. In our study, volcano extinction represents the "zero time" from which we consider long-term erosion.

After referring to the background information on the studied volcanoes, we present our methodology, and discuss the obtained results, focussing on quantitative relationships between edifice morphometry, erosion rate, erosion pattern and climate.

2. Geographic–geologic setting and geomorphic–climatic evolution

2.1. Geographic setting

The volcanoes studied here belong to the Central Volcanic Zone (CVZ) of the Central Andes (from 14 to 29°S) that formed by subduction of the Nazca plate (e.g. Stern, 2004). Today, the active volcanic arc of the CVZ is located in the Western Cordillera, but older Miocene to Quaternary volcanism covers a larger E–W extended area, particularly in the central part (Bolivian Altiplano) due to migrating arcs and changing slab dips (e.g. Isacks, 1988; Matteini et al., 2002; Stern, 2004; Mamani et al., 2010).

The 33 volcanoes included in this study are located in and around the Altiplano–Puna Plateau. Of these, 27 (between latitudes 16 and 22°S) rise from the Altiplano base level at 3800–4000 m a.s.l. Three volcanoes are located in the north at latitude ~14°S (in Ayacucho district of Peru, with a base level ≥4000 m a.s.l.), whereas another three are in the south at latitudes of 24 to 27°S in the Puna plateau, again almost at 4000 m base level elevation. Therefore, although the summit elevation of the volcanoes can be as high as 6500 m (ranging between 4776 and 6547 m a.s.l), their edifice heights from base to summit range from 600 to 2500 m, with the majority (20 out of 33) falling between 1000 and 2000 m (Table 1).

2.2. Formation and paleoclimate of the Altiplano–Puna plateau

Since the extreme arid climate of the Altiplano–Puna is an important constraint in this study, it is necessary to reiterate here briefly the most important geological features and climatic consequences of this orogenic plateau. Uplift and plateau-formation is related to the tectonic shortening of the Central Andes since ca. 25 Ma ago (see Allmendinger et al., 1997 and Gregory-Wodzicki, 2000 for reviews). Continued shortening concentrated in the Eastern Cordillera, and accelerated uplift of the plateau have occurred since the Late Miocene (ca. 10 Ma). During this time, an additional 2 to 3 km uplift resulted in the present elevation of the Altiplano and significant valley incision took place on its western flank (Wörner et al., 2000; Schildgen et al., 2007, 2009a,b, 2010; Thouret et al., 2007; Ehlers and Poulsen, 2009). In addition to such a tectonic forcing, arid climate and cooling down of the Peru–Chile oceanic current system may have also contributed to orogenic thickening and uplift by reducing sediment supply and also shear stresses between the convergent plates (Hartley, 2003; Lamb and Davis, 2003; Garcia-Castellanos, 2007).

Surface uplift enhanced the rain shadow effect by the Andes and changed atmospheric circulation patterns, resulting in progressively drier conditions and eventually hyperaridity in the Central Andes ca. 10–15 Ma ago (e.g. Ehlers and Poulsen, 2009). This aridification was synchronous with the uplift of the Altiplano–Puna plateau and is documented by >10 Ma old fossil landscapes along the Western Andean Escarpment (Wörner et al., 2000, 2002; Dunai et al., 2005). Aridity decreases slightly along a W–E gradient from the Atacama to the East Cordillera, and the uplift caused humid climates at the eastern margin of the orogen by concentrating moisture-bearing winds originating in the Amazon basin and the Atlantic (e.g. Strecker et al., 2007; Ehlers and Poulsen, 2009).

In the Quaternary, the Western Cordillera and the Altiplano were affected occasionally by cold and more humid climates resulting in glaciations at elevations >4200–4700 m (Clayton and Clapperton, 1997), and formation of a series of large paleolakes (e.g. Placzek et al., 2006, 2010). Since we attempt to quantify erosion patterns and rates over an area of more than 1000 km long and a >14 Ma time span, an important precondition for this study is that the general climate pattern, apart from minor, short-term fluctuations, remained largely unchanged since the mid-Miocene. This is proven by several lines of evidence summarized by Horton (1999) and Hoke and Garzione (2008).

Since at least the Late Miocene, extremely low erosion rates (<1–10 m/Ma) have occurred along the Coastal Cordillera (Dunai et al., 2005; Kober et al., 2007). Towards the Western Cordillera, erosion rates increase gradually to >10 m/Ma, as measured by cosmogenic nuclides (Kober et al., 2007) and on the basis of drainage basin analysis (Riquelme et al., 2008). Low erosion rates, endorheism, and a poorly developed drainage system left a largely undissected, low-relief fossil surface in particular on the western margin of the plateau (Wörner et al., 2000; Hartley and Chong, 2002; Hartley, 2003; Dunai et al., 2005; Alonso et al., 2006; Strecker et al., 2007).

At the same time, a north–south gradient has also developed along the western Andean margin with increased precipitation northward of the Arica Bend region (18°S; Horton, 1999; Klein et al., 1999; Placzek et al., 2006). This separates the low-erosion Altiplano–Puna plateau from the higher-erosion South Peruvian Cordillera (Horton, 1999). To the north, fluvial erosion is concentrated in a few large rivers that have created some of the deepest canyons in the world during the past 10 Ma (Thouret et al., 2007).

The age and location of the volcanoes studied here cover this time span of arid to hyperarid conditions (14 Ma to recent) and the N–S

Please cite this article as: Karátson, D., et al., Erosion rates and erosion patterns of Neogene to Quaternary stratovolcanoes in the Western Cordillera of the Central Andes: An SRTM DEM based analysis, Geomorphology (2011), doi:10.1016/j.geomorph.2011.10.010

extent from hyperarid Puna to less arid southern Peru (14°S to 27°S), allowing us to assess the effect of time and precipitation on erosion.

3. Methodology

Our method is based on the assumption that the present morphology of the selected, highly similar stratovolcanoes preserves some parts – typically, the middle and lower flanks – of the original volcanic edifice. A good fit of the middle and lower flanks to the ideal stratocone shape can be regarded as evidence for the former existence of a simple stratocone.

In fact, thanks to the low erosion rates and due to the fact that erosion has been confined predominantly to major dissecting valleys, even the strongly degraded Central Andean volcanoes preserve much of their middle and lower flanks showing almost intact planèzes (triangular remnants of original stratocone surfaces), e.g. at Cerro Anallajsi, Anocarire, Asuasuni, Chuquiananta, Huicso and Tunupa volcanoes, etc. (Table 1). Preservation of such original surfaces makes it possible to geometrically reconstruct the original, regular stratocone shape (Figs. 4, 5), which, in turn, is used to calculate the eroded volume and erosion rate subsequent to extinction.

SRTM digital elevation data have been used for the calculations. The original dataset was reprojected into UTM projection. Data processing was mostly performed in an ArcView GIS environment. Steps of the applied methodology are described below.

3.1. Fitting the ideal original cone morphology to the present relief

On the basis of the assumed petrological and volcanological similarities between the study examples, we postulate that the original (paleo)morphology of the selected simple cones was also similar. In order to numerically define an "ideal" morphology of a simple stratocone, we choose the most regular-shaped, most symmetric, least dissected, youngest volcano of the study area: Volcán Parinacota (Fig. 2a). Volcanological evolution of this stratovolcano is well known (Wörner et al., 1988, 2000; Clavero et al., 2004; Hora et al., 2007). Parinacota has a 150 ka lifetime, but the regular cone evolved over the last 50 ka on a base that is comprised by older domes and flow fields. With its highly symmetric cone shape, Parinacota volcano serves as a reference landform to assess the original shape and erosion of all the older regular-shaped volcanoes. We note that although the selection of simple stratovolcanoes leaves out irregular edifices such as clusters of domes (e.g. Taapaca: Wörner et al., 2000; Clavero et al., 2004) or volcanoes with a longer and more complex history (e.g. Aucanquilcha: Klemetti and Grunder, 2008), the calculated erosion rates should, in principle, be applicable to any other edifices in the region.

The radial symmetry of a volcanic cone, e.g. Parinacota (Fig. 2a), can be evaluated by arranging elevation data according to the horizontal distance from the cone centre (Fig. 2b). The cone centre is determined as the mean geometric centre of closed contour lines that encircle the volcano. Deviations from the mean elevation at a given distance from the cone centre are due either to outlying volcanic landforms (e.g. thick lava flows, adventive cones) or to erosional landforms (e.g. valleys, landslide scars). In order to simplify the point elevation "cloud" of the cone in Fig. 2b, we calculated the quartile elevation values (minimum, lower quartile, median, upper quartile, maximum) in each 50 m-wide horizontal ring (Fig. 2c). In the figure, it is clearly seen that the interquartile range is much smaller than the total range, suggesting that particular positive landforms should be cut off from the generalized shape of the volcano. However, in order to obtain the maximum extent of the pre-erosion surface, it is better to choose an upper envelope of the remaining elevation values at a given distance. We selected the upper quartile curve as best representing Parinacota's generalized profile (Fig. 2c). Then, this profile was divided into three sections and modelled by mathematical regression: 1) the summit section (e.g. crater) is represented by a constant elevation, 2) the upper cone section is represented by a linear equation (having a constant slope angle), and 3) the lower section is represented by a power function (i.e. decreasing slope angle towards the base of the volcano). In both the 2nd and 3rd sections, the fitting equations resulted in very high r^2 values (Fig. 2c), supporting the usage of these equations in further calculations.

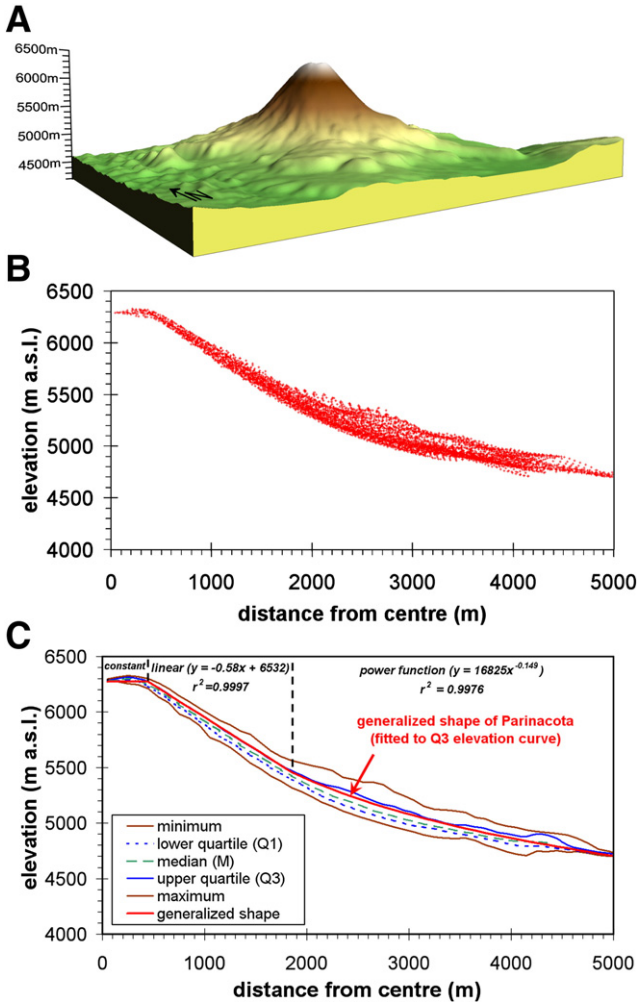

Fig. 2. Defining Parinacota's reference shape. (A) 3D model based on the 90 m resolution SRTM data. (B) Radial profiles from centre to base. (C) Statistical analysis of radial profiles to delineate the generalized shape reference. For further information, see text.

Certainly, selecting one volcano as an ideal landform should be tested on other examples in order to assess possible errors related to differences in initial cone morphologies. Therefore, Parinacota is compared in Section 3.3 to another highly symmetric, undisturbed conical edifice, Volcán Cotopaxi (Ecuador) (Garrison et al., 2006; Hall and Mothes, 2008).

Once the "ideal" cone profile is obtained, our method for volcano reconstruction – using the elevation data of the eroded volcanic cones – consists of five steps:

Step 1. Delimiting the cone and the apron boundaries. On most of the studied volcanoes, there is a remarkable slope angle pattern (Fig. 3) discriminating the cone (7–30°), the apron (1–7°), and the surrounding flat terrain (0–1°). Thanks to the careful selection of volcanoes without overlaps, regular aprons could have generally developed in all directions. The outer apron boundary indicates the area of the eruptive products issued out of the original volcano.

Step 2. Determining the centre of the cone. The cone centre is determined with the method presented for Parinacota, that is, by using the

Please cite this article as: Karátson, D., et al., Erosion rates and erosion patterns of Neogene to Quaternary stratovolcanoes in the Western Cordillera of the Central Andes: An SRTM DEM based analysis, Geomorphology (2011), doi:10.1016/j.geomorph.2011.10.010

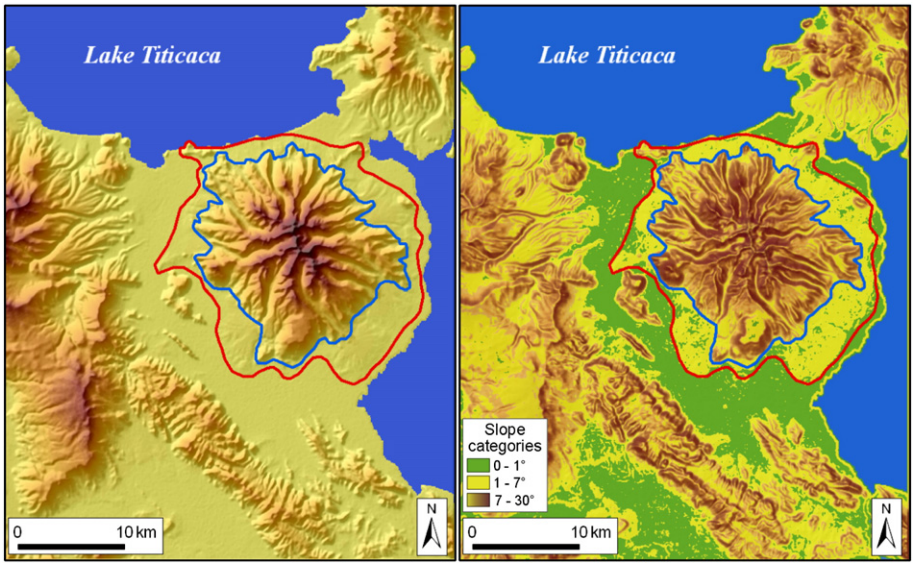

Fig. 3. Example how to delineate a volcano's boundaries: Volcan Japia (7.2 ± 0.09 Ma), which forms a peninsula within Lake Titicaca. As discussed in the text, there is a marked difference in slope angle between the cone (7–30°), the apron (1–7°) and the surrounding flat terrain (0–1°) defined by the blue and red line, respectively. In our work, the area of the volcano is defined by the outer apron boundary (blue line).

mean geometric centre of closed contour lines. However, since the oldest volcanoes can be highly degraded, only those contour lines are selected which encircle the whole central part of the volcano (i.e. small closed contours of individual peaks are neglected). The centre points of the closed contour lines are usually well concentrated, supporting our approach.

Step 3. Reconstructing the original cone profile. All pixel elevations are arranged according to their distance from the centre, and similarly to Parinacota, quartile values are calculated. Then, the "ideal" Parinacota profile is fitted to the actual volcano's upper quartile profile (Fig. 4). That segment is determined first in which the actual volcano's upper quartile profile shape ($Q_{3,i}$) is similar to that of Parinacota, meaning that the ridge heights (represented by the upper quartile) of this part of the volcano preserves the original morphology of the volcanic cone. This segment (from distance R_1 to distance R_2, see Fig. 4) is usually found at the middle/lower parts of the volcano. R_1 and R_2 are distances where the actual volcano's upper quartile curve and the generalized Parinacota shape curve diverge: left of R_1 and right of R_2 their slopes are significantly different. Then, the reference Parinacota profile (P_i) is vertically shifted by a value of X (henceforth called the "reconstructed profile"), so that the deviation between the corresponding segments will be minimal. The least squares method is used here, that is:

$$\sum_{i=R_1}^{R_2}\left(P_i + X - Q_{3,i}\right)^2 \tag{1}$$

is minimized. This condition is satisfied when X is the average of the deviations between Parinacota and the actual volcano elevations in the selected segment, that is:

$$X = -\frac{\sum_{i=R_1}^{R_2}\left(P_i - Q_{3,i}\right)}{n}, \tag{2}$$

where n is the number of increments between R_1 and R_2.

Of course, it may occur that fitting of the slopes is not possible due to slope deviations caused by lithological/eruptive characteristics, differential erosion, or a more complex, local pre-volcano topography. Thanks to our rigorous selection, non-fitting volcanoes were very few and these have been excluded from our analysis.

Step 4. Creating the DEM of the original cone. The elevation values of the central part of the volcano are increased to the "paleo" values according to their distance from the cone centre using the reconstructed profile. If the present topography is higher than the value calculated using the reconstructed profile (which usually occurs due to the aforementioned outlying landforms that are present at all volcanoes), then the present elevation is used. This way, the paleo-cone terrain is reconstructed as a new digital elevation model (Fig. 5).

Step 5. Determining the base level. The base level, an essential parameter for volumetric calculations, is defined as the average elevation of the apron boundary delimited in the first step. Assessment of errors related to uncertainties is given in Section 3.3.

3.2. Calculating volumes and erosion rates

In our study, volumes have been calculated within the delimited area using standard GIS methods. Paleovolume (1) is defined as the volume between the paleocone surface and the base level. Present volume (2) is defined as the volume between the present surface and the base level, whereas the volume removed by erosion (3) is the difference between (1) and (2). The degree of denudation (4) is calculated as the proportion of (3) and (1). Surface lowering (5) is the removed volume (3) divided by the area, therefore it characterizes the mean surface lowering by erosion over the area of the entire volcano and not that of a single topographic point. Erosion rate (6) is determined as the ratio of surface lowering and volcano age, for volcanoes where an age constraint is available.

3.3. Error assessment

Four types of errors are to be considered in connection with the above reconstruction method.

First, we show below that the relative volumetric error caused by the SRTM dataset inaccuracy is negligible. It is basically due to the fact that positive and negative errors are balanced in stratovolcano-scale volume calculations. This is mathematically proven based on two statistical theorems:

$$\sigma(cX) = |c|\cdot\sigma(X) \tag{3}$$

Please cite this article as: Karátson, D., et al., Erosion rates and erosion patterns of Neogene to Quaternary stratovolcanoes in the Western Cordillera of the Central Andes: An SRTM DEM based analysis, Geomorphology (2011), doi:10.1016/j.geomorph.2011.10.010

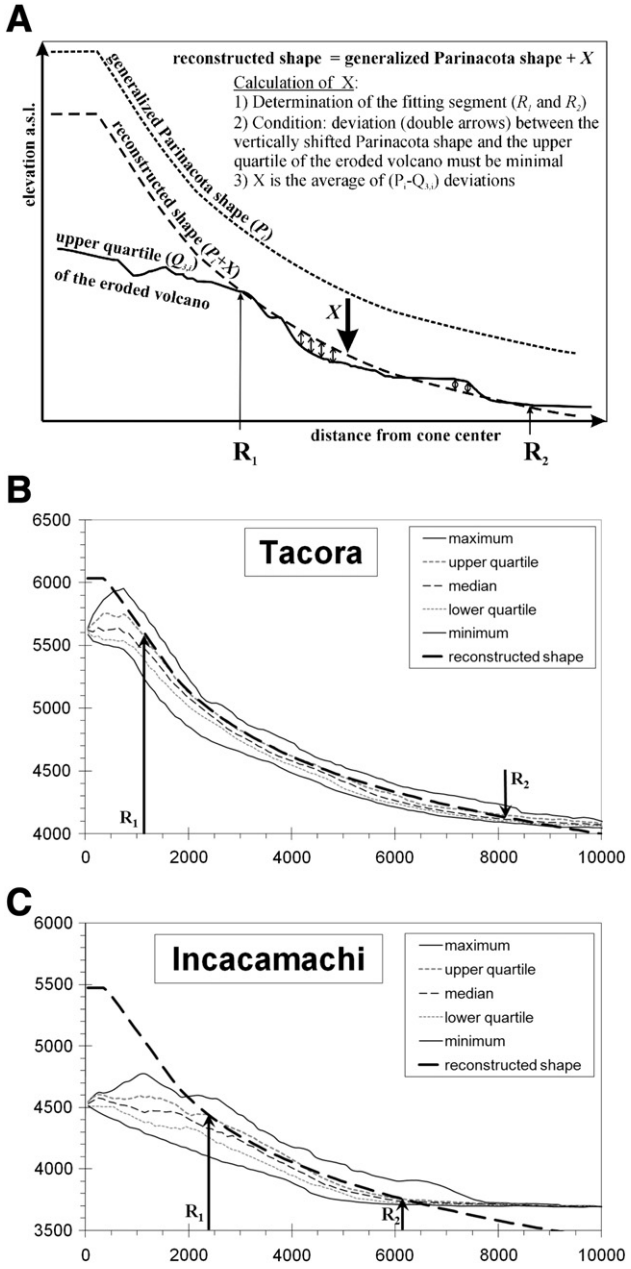

Fig. 4. Fitting Parinacota profile to actual eroded profiles. A: Methodology of least squares fit. Example volcano profiles are given for (B) a young slightly eroded (Tacora) and (C) an old significantly degraded (Incacamachi) edifice. Vertical exaggeration ~2.5.

$$\sigma(\bar{X}) = \frac{\sigma(X)}{\sqrt{N}} \tag{4}$$

where σ is standard deviation, c is a constant, X is a random variable, $\bar{X}$ is the mean of X and N is the number of data.

In the following, Δh is the height difference between SRTM and real height, ΔV is volume difference between volume calculated from SRTM and real volume, A_S is the area of an SRTM pixel (0.0081 km^2), N is the number of pixels within the area (A) of the studied landform.

Using these notations we can calculate the volume difference as follows:

$$\Delta V = \sum_{i=1}^{N} A_S \cdot \Delta h_i = A_S \cdot \sum_{i=1}^{N} \Delta h_i = A_S \cdot N \cdot \overline{\Delta h}. \tag{5}$$

Then 1σ-error of the volume is expressed as:

$$\sigma(\Delta V) = A_S \cdot N \cdot \sigma\left(\overline{\Delta h}\right) = A_S \cdot N \cdot \frac{\sigma(\Delta h)}{\sqrt{N}} = A_S \cdot \sqrt{N} \cdot \sigma(\Delta h) = \\ = A_S \cdot \sqrt{\frac{A}{A_S}} \cdot \sigma(\Delta h) = \sqrt{A_S} \cdot \sqrt{A} \cdot \sigma(\Delta h). \tag{6}$$

The area of the studied landforms is in the order of 100 km^2. $\sigma(\Delta h)$ is more difficult to determine. Based on large datasets, Rodriguez et al. (2005) found that it is ~5 m for all South America but for higher relief it is in the order of 10 m. Substituting these values into the equation we get

$$\sigma(\Delta V) = \sqrt{0.0081\ \text{km}^2} \cdot \sqrt{100\ \text{km}^2} \cdot 0.01\ \text{km} = 0.009\ \text{km}^3, \tag{7}$$

which is only 0.5% of the smallest eroded volume obtained (1.8 km^3, see Table 1). Since all other eroded volumes are larger, and present volumes as well as reconstructed volumes are much larger, it is concluded that the relative volumetric error due to the SRTM error is negligible in our study. However, while volume is linearly proportional to the studied landform area (A), its error is proportional to the square root of A (see Eq. (6)). As a consequence, the SRTM error estimated here cannot be neglected in volumetric studies on smaller-scale landforms.

Secondly, if the base level error is Δh_B and the area of the volcano is A, then both paleo- and present volumes have a maximum error of $A \cdot \Delta h_B$, whereas the eroded volume remains unaffected. The resulting error on the degree of denudation can be calculated (as seen in Table 1). Since the base level is determined as the average elevation of the apron boundary, due to Eq. (4) it is a statistically robust value with a small error only. Taking into consideration that the lower flanks of the apron have 1–2° slopes, respective vertical errors are 1.6–3.2 m/SRTM pixel. Therefore, in case of an ideal, (sub)horizontal substrate where boundary delimitation is highly reliable, the base level error is of the order of ~10 m. However, in case of more irregular, dipping substrate, or coalescent edifices, or presence of any extraneous terrain not belonging to the studied volcano, a larger error (~50 m) is more realistic. In the calculations, this larger error has been taken into account.

A third type of error may arise from the precision of fitting Parinacota's profile to the actual volcano's profile. Let R be the horizontal radius of the reconstructed paleocone surface and Δh_P the error of profile fitting. Then both paleo- and eroded volumes have an error of $R^2 \cdot \pi \cdot \Delta h_P$, contributing to the error of the degree of denudation (Table 1). Our experience suggests that the error of profile fitting is of the order of 10 m in the studied set of volcanoes. The sum of the second and third type of errors is presented in Table 1.

A fourth type of potential error may be due to differences in the original cone morphology (cf. Section 3.1), since our reference volcano (Parinacota) may not be entirely representative for the selected Central Andean stratovolcanoes, despite their apparent high similarities. Therefore, we compared the statistical elevation profiles of Parinacota to another active, regular, similar-sized Andean volcano, Cotopaxi (Northern Andes; Fig. 6). We found that the upper quartile elevation curve is indeed very similar to that of Parinacota, and the best-fit linear and power functions result in highly similar parameters as well as high correlation coefficients. (Note that a vertical shift of the curve was applied since Parinacota is ~500 m higher than Cotopaxi.) In comparison, when calculating the volumetry for the generalized shapes of Parinacota and Cotopaxi, we obtained the following differences: below 8100 m radius, the difference is smaller than 1 km^3; above this value (at lower edifice elevations) the difference is increasing due to shape function differences and the much larger area of aprons. For example, at 10,000 m radius, the difference is ~4 km^3. However, since at

Please cite this article as: Karátson, D., et al., Erosion rates and erosion patterns of Neogene to Quaternary stratovolcanoes in the Western Cordillera of the Central Andes: An SRTM DEM based analysis, Geomorphology (2011), doi:10.1016/j.geomorph.2011.10.010

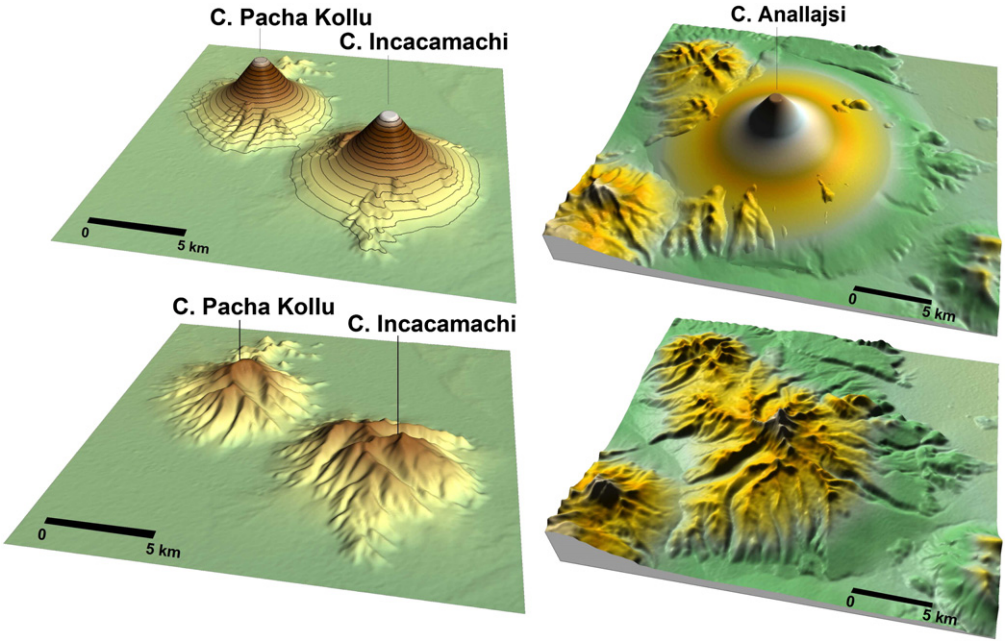

Fig. 5. Restored model morphologies of original volcanic cones based on the DEM reconstruction (left: Pacha Kollu; right: Cerro Anallajsi).

most studied volcanoes the reconstructed cone radius remains below 8000 m, the volumetric differences are expected to be less than 1 km^3.

3.4. Circularity of the volcanoes

In order to characterize the erosion pattern of the volcanoes, beside standard DEM visualization techniques (3D, shading, slope, aspect), ridge and valley detection filters (those in Karátson et al., 2010b) were also used to enhance pattern recognition. In addition, for morphometric characterization, the circularity of closed contour lines was also calculated (taking into account only the contours which encircle the whole central part of the volcano).

Circularity (C) is defined in our study by the following formula:

$$C = \frac{\sqrt{A/\pi}}{P/2\pi} \tag{8}$$

where A is the area enclosed by the contour and P is the perimeter (length) of the contour. Circularity is 1 for any circle, and the more dissected the contour, the smaller its circularity. In fact, this parameter is the reciprocal of the dissection index used in Wright et al. (2006). Although the circularity value is sensitive to elongation as well, in case of radially symmetrical stratocones, this does not greatly influence the results. Thus, the circularity is supposed to be close to 1 for a young volcano, and either the mean circularity of the whole cone or the circularity of selected contour levels may be suitable to detect the effects of erosion due, above all, to valley dissection.

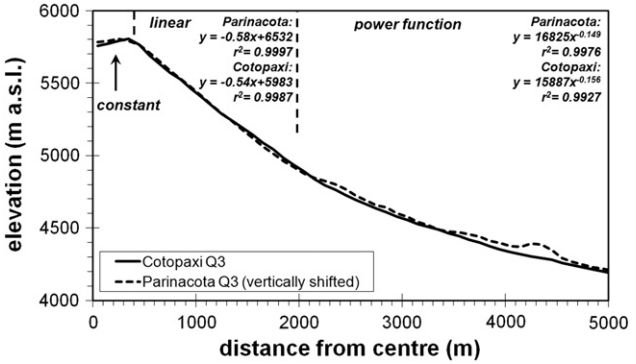

Fig. 6. Comparison of profiles of two highly symmetric stratovolcanoes: Parinacota and Cotopaxi. Elevations for Parinacota have been vertically shifted in order to account for different base level elevations of these two stratovolcanoes. Note the excellent agreement between the two models, which validates the usage of the Parinacota reference shape to other Central Andean volcanoes.

4. Model results

Geographic data of individual stratovolcanoes (locality, absolute and relative elevation, base level), age constraints, and results of volumetric and erosion rate calculations, are given in Table 1. Highlighted are the most important results: the degree of denudation and erosion rate.

The degree of denudation of the studied volcanoes is in the range of 0–50%, that means that within the studied time span (~14 Ma) only up to half the original volcanic edifice has been removed by erosion. The average degree of denudation is 22%. The relatively small values support and quantify Horton's (1999) suggestion that Mid-Miocene volcanoes in the Bolivian Altiplano "retain their original volcanic morphology" (…), and "remain virtually unaltered from their original states, suggesting extremely low rates of denudation" (cf. also de Silva and Francis, 1991).

The erosion rates calculated for volcanoes with age constraints highly depend on volcano age. A distinct group, the three Quaternary volcanoes, shows very high but abruptly decreasing erosion rates with age (112 to 66 m/Ma). By contrast, the remaining eight volcanoes are characterized by more similar and much lower erosion rates, ranging from 7 to 25 m/Ma, apparently independent of volcano age. Evaluation of this dual behaviour, as well as minor but systematic differences within these low erosion rates, are addressed in the Discussion section.

In Fig. 7, relative height (H) is plotted against the degree of denudation to show the correlation between the reduction in edifice height and volume loss by erosion. There is a moderate correlation ($r^2 = 0.68$, $p = 0.0000$), i.e. edifice height is progressively smaller with denudation. However, the reduction in elevation is not necessarily a linear function of erosion age. Rather, by analysing a great

Please cite this article as: Karátson, D., et al., Erosion rates and erosion patterns of Neogene to Quaternary stratovolcanoes in the Western Cordillera of the Central Andes: An SRTM DEM based analysis, Geomorphology (2011), doi:10.1016/j.geomorph.2011.10.010

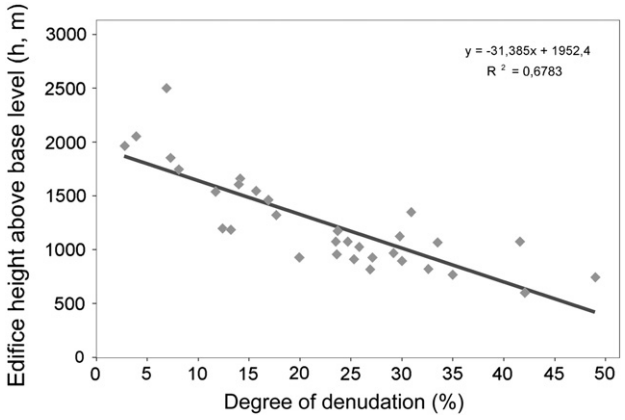

Fig. 7. Edifice height vs. degree of denudation.

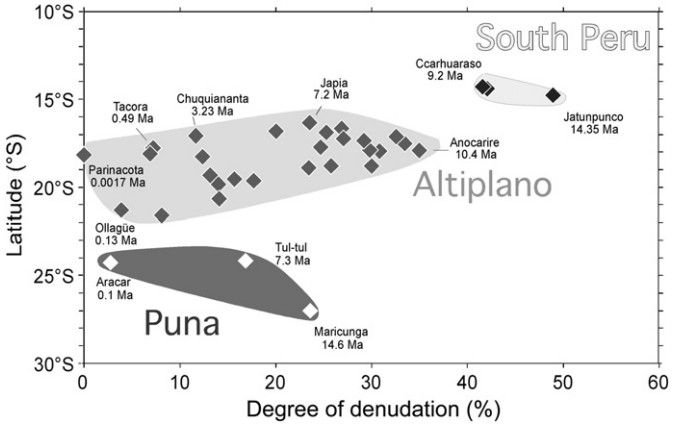

Fig. 9. Latitude vs. degree of denudation.

number of volcano profiles, we found that the erosional history of volcanoes follows specific patterns through well-defined stages. We will further address this question in the Discussion section.

In Fig. 8, the degree of denudation vs. age plot is presented for the 11 volcanoes having radiometric age constraints. The correlation for all volcanoes is relatively good ($r^2 = 0.76$, $p = 0.0005$), although it includes some volcanoes that were eroded under different climates (especially different precipitation conditions, as described in 2.2). Therefore, it is worth excluding the hyperarid Puna volcanoes (Aracar, Maricunga and Tul-tul), as well as those in South Peru (Ccarhuaraso and Jatunpunco), which receive higher precipitation at present. As a result, considering only volcanoes that were eroded under similar climatic conditions, there is a significant improvement in the correlation ($r^2 = 0.97$, $p = 0.0003$). Since the p-values are less than 0.01 in all cases, these relationships are all statistically significant at the 99% confidence level. Implications to climatic patterns as well as long-term landscape evolution are given in the Discussion section.

In Fig. 9, the degree of denudation is plotted against latitude, along with ages where available. In accordance with the degree of denudation vs. age plot, two trends can be distinguished: (1) volcanoes located in the arid Altiplano, including those in South Peru under more humid climate, and (2) volcanoes of the hyperarid Puna plateau. The former group contains the majority of the studied volcanoes, which are roughly older and more degraded from S to N (between latitudes ~20° and 14°). Therefore, as already seen in Fig. 8, volcanoes of South Peru which fit to the general Altiplano trend show the highest degradation. By contrast, the Puna volcanoes seem to follow a different erosional trend: during the same period (i.e. 14 Ma, the whole time span investigated) their degradation has obviously been less. Here, the oldest volcano, the 14.6 Ma-old Maricunga, exhibits half the degree of denudation compared to the same-aged Jatunpunco in South Peru. Since apart from climate, all volcanological, geomorphological and topographical parameters are thought to be similar for the selected volcanoes, our results show that (1) precipitation and erosion rates are strongly correlated, and (2) this correlation – similarly to the present climate gradient – existed for a long time span (>10 Ma).

Finally, in order to constrain the changes in volcano morphology with time, we present two plots of circularity (Fig. 10). The mean circularity values (Fig. 10a) show a general decrease of circularity with the degree of denudation (which roughly correlate with time). However, the correlation between the mean circularity and the degree of denudation is moderate ($r^2 = 0.58$, $p = 0.0000$), which may be due to the specific changes of the stratocone landform, reflected by individual circularity values at given heights (Fig. 10b).

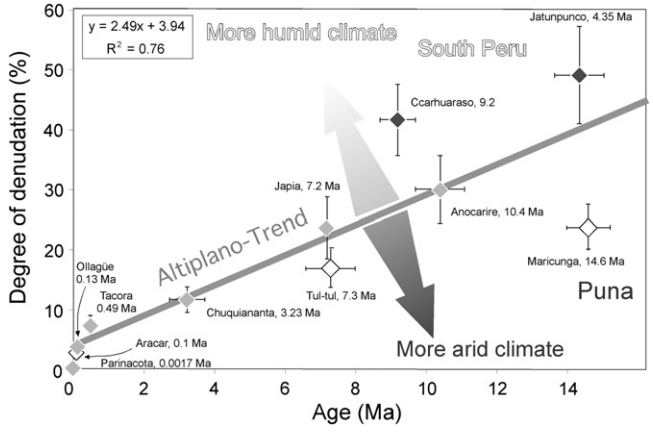

Fig. 8. Degree of denudation vs. volcano age (dates were used as starting time for erosion, see text).

5. Discussion

5.1. Volcano size

The selected 33 stratovolcanoes represent edifices with variable sizes: the calculated original volumes range from 33 to 295 km^3. Within this range, smaller-volume volcanoes are more abundant (<80 km^3: 19, 80–120 km^3; 7, >120 km^3; 7 volcanoes, see Table 1). As expected, reconstructed volcano volumes are not related to latitudinal position, since there is no correlation between volume and latitude ($r^2 = 0.06$).

The good fit of Parinacota's elevation profile to most of the studied volcanoes implies that all selected volcanoes may have had similar cone shape, regardless of the final volume they reached during evolution. This conclusion is also supported by the similarity between Parinacota and Cotopaxi. Larger volume cones may have evolved by constructing a progressively larger apron. For example, the case of Sajama shows that a relatively small increment in height (see, for example, its relative height compared to Parinacota or Tacora) is coupled with a highly increased areal extent of the volcano periphery.

Some of the youngest studied volcanoes of the Central Andes have a relative edifice height up to 2.5 km, and all the Quaternary volcanoes have large height/diameter (H/D) ratios of 0.10–0.15 (Table 1), corresponding to similar H/D ratios at active volcanoes worldwide (Wood, 1978; Grosse et al., 2009). By contrast, the majority of the volcanoes included in this study show much smaller H/D values (the average is 0.08), in accordance with their older ages and related erosional degradation (Fig. 7).

Please cite this article as: Karátson, D., et al., Erosion rates and erosion patterns of Neogene to Quaternary stratovolcanoes in the Western Cordillera of the Central Andes: An SRTM DEM based analysis, Geomorphology (2011), doi:10.1016/j.geomorph.2011.10.010

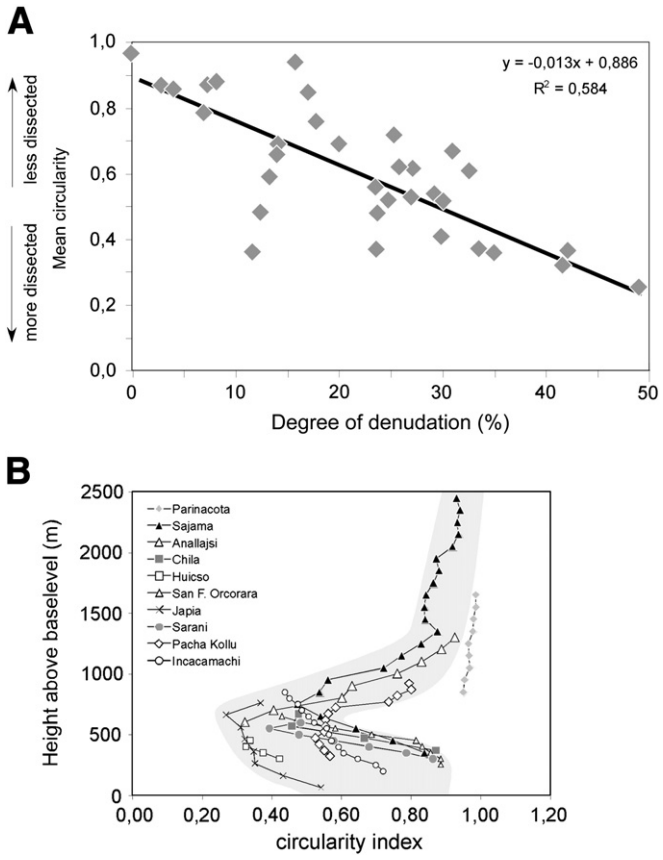

Fig. 10. Circularities of selected Central Andean stratovolcanoes. A: Mean circularity index. B: Contour line based circularity values. For explanation and discussion, see text.

5.2. Erosion controlled by age and climate

The degree of denudation (vs.) age correlation as well as the correlation with latitude enable us to establish relationships between erosion rates, age, and general rainfall patterns.

The degree of denudation becomes larger for the progressively older Altiplano volcanoes (roughly from south to north), including the present-day more humid South Peruvian volcanoes as well (Figs. 8, 9). This is a well-defined trend over the entire region, with the exception of the three volcanoes of the southernmost, hyperarid Puna plateau which exhibit lower denudation with respect to their age.

Denudation time-scales however are better illustrated by erosion rate magnitudes (Table 1). As described in the Methodology section, erosion rates have been calculated for volcanoes with age constraints from surface lowering, and hence represent average values for the whole area of the given volcano.

First, we have to distinguish the much higher short-term (<100 ka) initial erosion from the lower long-term (>1 Ma) rates. Notably, this higher erosion rate on younger volcanoes is not an artefact caused by the higher degree of preservation of younger correlative sediments (e.g. as indicated by Willenbring and von Blanckenburg, 2010). Instead, our estimates are a direct measure of erosion and not calculated from sediments.

Typically, erosion rates of young volcanoes all over the world show very high values. As has been previously shown (e.g. Ruxton and McDougall, 1967; Drake, 1976; Ollier, 1988; Karátson, 1996) initial erosion rates up to 1000 mm/ka (i.e. 1000 m/Ma) or higher can be attributed to the presence of unconsolidated volcanic material and the lack of vegetation on steep (up to ~30°) slopes. However, over a short time (~10–100 ka), high erosion rates slow down due to the removal of loose tephra, the consolidation/compaction of pyroclastic deposits, as well as the stabilization of drainage (Ollier, 1988; Karátson, 1996). Therefore, although the Central Andean volcanoes show a good linear correlation between denudation ratio and age over the long term (Fig. 8), the first segment of the regression is not linear, even if this is a very short period relative to the 10 Ma-long time-scale.

As seen in Table 1, out of the Quaternary volcanoes of the Altiplano–Puna, Volcán Ollagüe and Volcán Tacora have high erosion rates of 112 and 66 m/Ma, respectively, in accordance with their age relation (the older Tacora has lower erosion rate). The third youngest volcano, Cerro Aracar has no direct radiometric age, but with reference to a Bulletin of the Global Volcanism Network report (04/1993 BGVN 18:04), it is constrained to Late Quaternary. Assuming a 0.1 Ma age, it also gives a high erosion rate of 94 m/Ma, which fits to the others. Although erosion rate differences can be partly attributed to lithology (i.e. contrasting erodibility), we suggest that the high but rapidly decreasing erosion rates reflect chiefly the progressive removal of loose material, and the stabilization of erosion on progressively more gentle-sloped volcano flanks.

The much lower and more constant long-term erosion rates (Table 1) seem to be determined mostly by climate. Variable climate from the core of the Atacama desert to the surrounding less arid areas is a more significant factor relative to lithology, as it was also pointed out by Kober et al. (2007). In fact, in a worldwide comparison, the erosion rates obtained in our study (13.5 m/Ma on average for the >3 Ma-old volcanoes) are significantly lower than those calculated for moderate continental to semihumid climates (e.g. Ollier, 1988; Summerfield, 1991; Karátson, 1996; Hayashi et al., 1999).

Out of the studied pre-Quaternary volcanoes, the Pliocene Cerro Chuquiananta volcano (3.2 Ma) shows a moderate erosion rate of 25 m/Ma, whilst all other Miocene volcanoes (with >7 Ma ages) have even lower erosion rates (11.8 m/Ma on average). These low rates are in good agreement with previous erosion rate calculations for the Altiplano–Puna region summarized in Section 2.2.

The smallest erosion rates of the studied volcanoes are derived for the hyperarid Puna volcanoes (Cerro Maricunga: 7.1 m/Ma; Cerro Tul-tul: 8.7 m/Ma; Table 1). By contrast, the South Peruvian volcanoes under semi-humid climate, although they largely fit to the general trend of Central Andean volcanoes (Figs. 8, 9), exhibit slightly higher erosion rates (Cerro Jatunpunco: 13.1 m/Ma, Cerro Ccarhuaraso: 21.6 m/Ma). In spite of these small differences, long-term erosion rates are still relatively similar between the regions north and south of the Arica Bend (17°30′) (Figs. 8, 9). Note, however, that some of the studied volcanoes are significantly older than the beginning of the last phase of Andean uplift (~10 Ma). That event triggered the incision of deep canyons in the western Andean margin, suggesting increased erosion power and erosion rates on the Western Cordillera in South Peru (Thouret et al., 2007; Schildgen et al., 2010) as well as in North Chile (Wörner et al., 2000; Riquelme et al., 2008). Moreover, the Quaternary erosion was also increased by glaciation and glacial incision in many places, and occasional extreme erosion occurred under wet climates in interglacials (Clayton and Clapperton, 1997; Ammann et al., 2001). Therefore, the relatively high erosion rates (13–22 m/Ma) of the older volcanoes (14–10 Ma) in South Peru average out more recent higher and old (pre-uplift) possibly lower erosion rates (which may have existed due to the arid climate conditions that pre-date even the oldest volcanoes, cf. Alpers and Brimhall, 1988; Hartley, 2003). Similar balancing of short-term and/or regional climatic fluctuations can be valid for large areas, in agreement with Kober et al.'s (2007) statement that "Miocene landscapes are not static but dynamic features though with low geomorphic process rates". However, the overall correlations that we observe are still maintained despite these local and temporal fluctuations. First, even in South Peru, volcanic edifices have not yet been significantly incised by the <10 Ma-old deep canyons (Volcán Solimana being the only exception). Second, temporal fluctuations are averaged out over longer

Please cite this article as: Karátson, D., et al., Erosion rates and erosion patterns of Neogene to Quaternary stratovolcanoes in the Western Cordillera of the Central Andes: An SRTM DEM based analysis, Geomorphology (2011), doi:10.1016/j.geomorph.2011.10.010

(ca. >3 Ma) time spans. Finally, glaciation has remained generally a relatively superficial and short-lived erosive power due to the small glacier size and volume in this arid climate. Alpine-type dissection with spurs and ridges, which are frequently observed in deeply eroded volcanic landforms in the Southern Volcanic Zone, are conspicuously absent in the Central Andes.

5.3. Age estimation

The degree of denudation vs. age correlation (Fig. 7) makes it possible to estimate the "erosional" age for Central Andean volcanoes based on morphology. Namely, the inverse correlation provides the approximate time elapsed since the extinction of the volcano from which the degree of denudation was calculated (Table 1). The calculation equation is based on all radiometric ages, involving both the Altiplano and Puna volcanoes. Because the former have larger and the latter smaller degrees of denudation with respect to the average (see above), Puna erosional ages are overestimated relative to the radiometric ages (by 0.2, 2.2 and 7.0 Ma) while South Peruvian erosional ages are underestimated (by 4.9 and 2.4 Ma). However, for the remaining 5 Altiplano volcanoes, the age uncertainty is relatively small (<1.1 Ma). Therefore, such a geomorphological dating tool could be used as a first approach to constrain the age of similar simple stratovolcanoes that have been eroded under similar climatic conditions.

5.4. Surface evolution of the stratovolcanoes forced by climate

General rules of erosion based on morphometric correlations, analysis of circularity, as well as interpretation of a great number of individual volcano profiles enable us to infer long-term landscape evolution patterns of the studied stratovolcanoes.

We have seen in Fig. 7 that the relative volcano height and denudation ratio are inversely correlated, but the correlation is only moderately good ($r^2 = 0.68$). This implies that in addition to the general long-term erosional lowering of the surface, there may be important qualitative changes during the degradation of the volcanoes. Obviously, the most remarkable changes have been due to Quaternary glaciations that resulted in short-lived accelerated erosion, especially valley development. As pointed out by several authors (e.g. Clayton and Clapperton, 1997), successions of typical U-shaped valleys with moraines at a number of degraded volcanoes of the Altiplano–Puna region indicate repeated glacier advances down to 4000 m on the Altiplano and the Western Cordillera. Typically, these valleys excavate deeply, preferentially into the upper volcano flanks and have no drainage outward at present. Remnants of outlet valleys, if any, have been obscured since then. Under the arid climate of the Altiplano, these glacial valleys are fossil landforms on the volcanoes, further masked by deposits from ongoing (although slow-rate) areal erosion processes such as slumping, creep and occasional slope failure (e.g. Strasser and Schlunegger, 2005; Alonso et al., 2006). By contrast, under the more humid climate of South Peru, volcanic terrains have been more deeply incised by canyons and normal, dendritic drainage pattern, which overprinted radial systems of glacial valleys (e.g. Cerro Ccarhuaraso).

On the basis of the typical erosional signal, i.e. the presence of a number of fossil, bottleneck-shaped glacial valleys in radial directions on many Central Andean volcanoes, we propose the term "edelweiss" volcano (Fig. 11). This pattern is particularly remarkable on satellite images and ridge-enhanced digital elevation models. This stage can be a peculiar remnant stage of volcano erosion (Macdonald, 1972; Ollier, 1988; Davidson and de Silva, 2000), roughly corresponding to the planèze stage under more humid climates. In areas with heavier rainfall (e.g. in South Peru), such a pattern has been modified and ultimately destroyed by the evolving normal dendritic drainage (Fig. 11). As far as long-term surface evolution is concerned, the presence of glacial valleys is just an overprinting of much older histories back to Pliocene or even Miocene times. The longer-term erosional dissection, although mostly obscured, is still reflected by the changes of circularity of the stratovolcanoes. Namely, high circularity values of active or dormant volcanoes (0.8–1: e.g. Parinacota) decrease to 0.3 for the oldest, most degraded ones (e.g. Cerro Huicso, Cerro Jatunpunco: Fig. 10a), which reflects the increasing role of dissection. However, the correlation is only moderate, that is mostly due to the peculiar circularity trends at given elevations (Fig. 10b). In the summit region, high circularity is typical, on the mid-flanks circularity is rapidly decreased, while toward the apron, circularity improves

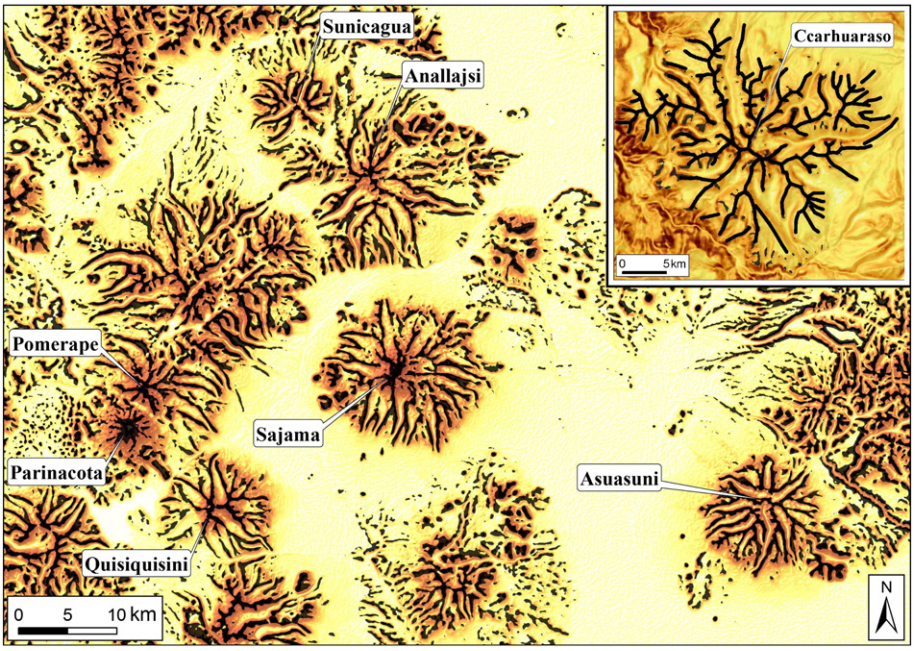

Fig. 11. "Edelweiss" volcanoes of the arid Altiplano (in particular, Sajama, Quisiquisini, Asuasuni, Sunicagua) showing fossil glacial valleys. By contrast, the relief of Ccarhuaraso in more humid South Peru may have been overprinted by a subsequent dendritic pattern. SRTM DEM-based, slightly shaded slope maps with ridge enhancement were produced by using median difference filtering method (for details of ridge enhancement, see Karátson et al., 2010b).

Please cite this article as: Karátson, D., et al., Erosion rates and erosion patterns of Neogene to Quaternary stratovolcanoes in the Western Cordillera of the Central Andes: An SRTM DEM based analysis, Geomorphology (2011), doi:10.1016/j.geomorph.2011.10.010

again. We suggest that this regular change reflects the peculiar erosional dissection of the Central Andean volcanoes under arid climate conditions. Namely, the valleys on the volcanoes' mid-flanks (i.e. ancient fluvial valleys overprinted by glaciation) dissect and degrade the volcano, resulting in a lower circularity, while at the lower flanks and the apron, lower stream power (due to smaller topographic gradient and limited discharge) impedes valley incision and propagation. Sedimentation on the lower flanks also contributes to making the apron circular again.

Based on the above evaluation of degradation and valley development, we outline an evolutionary model for the degradation of the studied Central Andean volcanoes (Figs. 11, 12), to explain the observed discontinuous summit lowering despite continuous degradation:

(1) Intact volcano (active or dormant) stage, best represented by Parinacota, a simple, highly circular, symmetrical crater-topped stratovolcano.
(2) A still perfect cone-shaped, but slightly to moderately eroded volcano with developing valleys on the flanks and initial planèzes, without crater (e.g. Sajama) or with an erosionally enlarged crater/central depression.
(3) A considerably eroded volcano with a truncated upper cone due to large valleys, which are possibly glacially modified. This type of volcano already experienced significant lowering, but still retains a large proportion of its original volume and preserves well-developed planèzes at the lower flanks. Examples are Cerro Asuasuni and Cerro Mamuta (~9 to 10 Ma old, Mortimer et al., 1974). The latter is an excellent example but could not be included in our study because of its tilted base.
(4) A deeply eroded cone with remnants of planèzes and remnant peaks in the centre (e.g. Cerro Anallajsi), that may remain high at its centre for a long time, but the overall degradation resulted in a significant volume loss.
(5) A "valley-stage" remnant volcano, where headward erosion and the coalescence of large valleys (either of glacial or fluvial origin) resulted in a completely degraded, lowered summit (e.g. Cerro Huicso and Cerro Jatunpunco); here, the volcanic cone can be distinguished rather in plan view than in cross-section.

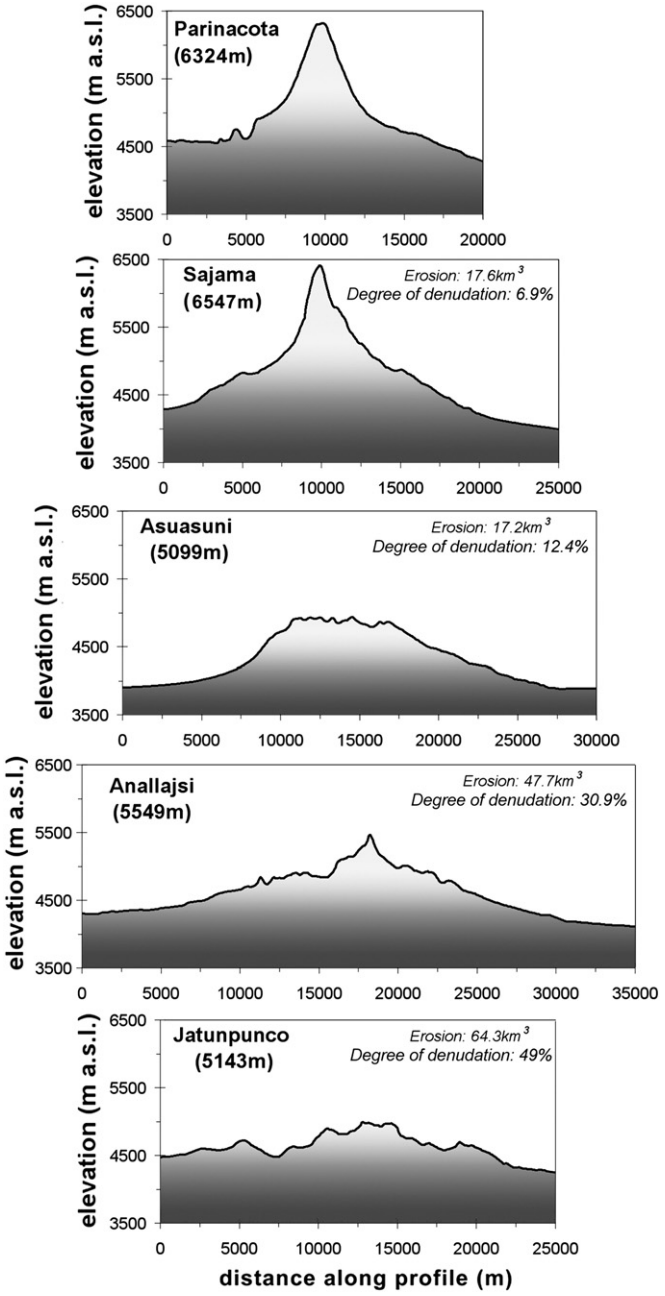

Fig. 12. Erosion history of Central Andean stratovolcanoes in typical stages on five representative profiles. Scale is the same. Vertical exaggeration is ~5. For explanation, see text.

6. Conclusions

The Western Cordillera of the Central Andes offers a unique opportunity to quantify erosion processes, and infer erosion patterns and rates of stratovolcanoes. The low erosion results mostly from the predominant, long-term arid climate. By using an advanced morphometry, we obtained values for the degree of denudation for 33 Mid-Miocene to recent stratovolcanoes, and determined erosion rates for those which have radiometric age constraints.

Degree of denudation, that is, volume loss, is 22% on average and up to 50% as a maximum. It means that more than half of the original volume has been preserved even for the Miocene edifices. Surface lowering averaged for volcano area is ~90 m on average and ranges to 200 m. These relatively small figures are reflected by low erosion rates of the order of ~10 m/Ma obtained for the older (>3 Ma) volcanoes. These low average rates may have been in operation since the onset of the arid climate (10–15 Ma) over the Altiplano–Puna Plateau. In comparison, slightly higher erosion rates (up to ~20 m/Ma) typify the South Peruvian volcanoes, which are located under more humid climate conditions. The obtained long-term erosion rates are remarkably distinct from the much higher short-term erosion rates (66–112 m/Ma) which characterize the younger (≤0.5 Ma) volcanoes. These high rates are typical of recent volcanoes worldwide having unconsolidated erodible surfaces. We suggest that since climate is the major factor determining erosion, the obtained erosion rates are applicable to other volcano types as well.

A geomorphologic dating for remote volcanoes with unknown eruptive age is provided by the degree of denudation ratio vs. age correlation, constraining the time elapsed since volcanic activity. However, this calculation can be applied reliably (with an error of ~1 Ma) only for the Atiplano region.

Finally, we outline a general erosional history for the volcanoes of the Western Cordillera, in particular the Altiplano Plateau. These volcanoes develop a peculiar star- or "edelweiss"-like ridge-and-valley pattern, characterized by a systematic circularity vs. elevation distribution. We suggest that valley evolution has resulted in temporally uneven surface lowering. In case of pre-Quaternary volcanoes, the glacial valleys overprinted older valleys, and conversely, glacial valleys could have been destroyed by a dendritic drainage pattern under more humid climates (in South Peru).

Please cite this article as: Karátson, D., et al., Erosion rates and erosion patterns of Neogene to Quaternary stratovolcanoes in the Western Cordillera of the Central Andes: An SRTM DEM based analysis, Geomorphology (2011), doi:10.1016/j.geomorph.2011.10.010

Acknowledgements

The research was funded by a Humboldt Fellowship (3.3-UNG/1115049 STP) to D. K. in 2008–2010. Some aspects of the work and interpretation of results were clarified during fruitful discussions in volcano geomorphology sessions at EGU 2010 and 2011 in Vienna. The authors thank three anonymous reviewers for their helpful comments on the manuscript. Andrew Plater is acknowledged for editorial handling.

References

Allmendinger, R.W., Jordan, T.E., Kay, S.M., Isacks, B.L., 1997. The evolution of the Altiplano–Puna Plateau of the central Andes. Annual Review of Earth and Planetary Sciences 25, 139–174.

Alonso, R.N., Bookhagen, B., Carrapa, B., Coutand, I., Haschke1, M., Hilley, G.E., Schoenbohm, L., Sobel, E.R., Strecker, M.R., Trauth, M.H., Villanueva, A., 2006. Tectonics, climate, and landscape evolution of the Southern Central Andes: the Argentine Puna Plateau and adjacent regions between 22 and 30°S. In: Oncken, O., Chong, G., Franz, G., Giese, P., Götze, H.J., Ramos, V.A., Strecker, M.R., Wigger, P. (Eds.), The Andes — active subduction orogeny: Frontiers in Earth Sciences, Vol. 1. Springer, pp. 265–283.

Alpers, C., Brimhall, G., 1988. Middle Miocene climatic change in the Atacama Desert, northern Chile: evidence from supergene mineralization at La Escondida. Bulletin Geological Society of America 100 (10), 1640.

Ammann, C., Jenny, B., Kammer, K., Messerli, B., 2001. Late Quaternary glacier response to humidity changes in the arid Andes of Chile (18–29°S). Palaeogeography, Palaeoclimatology, Palaeoecology 172, 313–326.

Bellon, H., Lefèvre, R., 1977. Spectre d'âges radiométriques du volcanisme cénozoïque du Pérou central (région de Castrovirreyna–Ayacucho–Nazca). Réunion Annuelle des Sciences de la Terre, 5 (58 pp.).

Berry, P.A.M., Garlick, J.D., Smith, R.G., 2007. Near-global validation of the SRTM DEM using satellite radar altimetry. Remote Sensing of Environment 106, 17–27. doi:10.1016/j.rse.2006.07.011.

Bolch, T., Kamp, U., Olsenholler, J., 2005. Using ASTER and SRTM DEMs for studying geomorphology and glaciers in high mountain areas. In: Oluic, M. (Ed.), New Strategies for European Remote Sensing (Proceedings of the 24th Meeting European Association of Remote Sensing Laboratories, 2004, Dubrovnik, Croatia), pp. 119–127 (S.).

Charrier, R., Chávez, A.N., Elgueta, S., Hérail, G., Flynn, J.J., Croft, D.A., Wyss, A.R., Riquelme, R., García, M., 2004. Rapid tectonic and paleogeographic evolution associated with the development of the Chucal anticline and the Chucal–Lauca Basin in the Altiplano of Arica, northern Chile. Journal of South American Earth Sciences 19, 35–54.

Clavero, J.E., Sparks, S.J., Pringle, M.S., Polanco, E., Gardeweg, M.C., 2004. Evolution and volcanic hazards of Taapaca Volcanic Complex, Central Andes of Northern Chile. Journal of the Geological Society of London 161, 603–618.

Clayton, J.D., Clapperton, C.M., 1997. Broad synchrony of a Late-glacial glacier advance and the highstand of palaeolake Tauca in the Bolivian Altiplano. Journal of Quaternary Science 12 (3), 169–182.

Crippen, R.E., Hook, S.J., Fielding, E.J., 2007. Nighttime ASTER thermal imagery as an elevation surrogate for filling SRTM DEM voids. Geophysical Research Letters 34, L01302. doi:10.1029/2006GL028496.

Davidson, J., de Silva, S.L., 2000. Composite volcanoes. In: Sigurdsson, H. (Ed.), Encyclopedia of Volcanoes. Academic Press, pp. 663–682.

de Silva, S.L., Francis, P.W., 1991. Volcanoes of the Central Andes. Springer, Berlin. (216 pp.).

Drake, R.E., 1976. Chronology of Cenozoic igneous and tectonic events in central Chilean Andes — latitudes 35°30 to 36°. Journal of Volcanology and Geothermal Research 1, 265–284.

Dunai, T., González López, G., Juez-Larré, J., 2005. Oligocene–Miocene age of aridity in the Atacama Desert revealed by exposure dating of erosion-sensitive landforms. Geology 33, 321–324.

Ehlers, T., Poulsen, C., 2009. Influence of Andean uplift on climate and paleoaltimetry estimates. Earth and Planetary Science Letters 281, 238–248.

Farr, T.G., et al., 2007. The shuttle radar topography mission. Reviews of Geophysics 45, RG2004. doi:10.1029/2005RG000183.

Garcia-Castellanos, D., 2007. The role of climate during high plateau formation. Insights from numerical experiments. Earth and Planetary Science Letters 257, 372–390.

Garreaud, R.D., Molina, A., Farias, M., 2010. Andean uplift, ocean cooling and Atacama hyperaridity: a climate modeling perspective. Earth and Planetary Science Letters 292, 39–50.

Garrison, G., Davidson, J., Reid, M., Turner, S., 2006. Source versus differentiation controls on U-series disequilibria: insights from Cotopaxi Volcano, Ecuador. Earth and Planetary Science Letters 244, 548–565.

Gregory-Wodzicki, K.M., 2000. Uplift history of the Central and Northern Andes: a review. Geological Society of America Bulletin 112 (7), 1091–1105.

Grosse, P., van Wyk de Vries, B., Petrinovic, I., Euillades, P.A., Alvarado, G.E., 2009. Morphometry and evolution of arc volcanoes. Geology 37, 651–654. doi:10.1130/G25734A.1.

Hall, M., Mothes, P., 2008. The rhyolitic–andesitic eruptive history of Cotopaxi volcano, Ecuador. Bulletin of Volcanology 70, 675–702.

Hartley, A., 2003. Andean uplift and climate change. Journal of the Geological Society 160, 7–10.

Hartley, A.J., Chong, G., 2002. Late Pliocene age for the Atacama Desert: implications for the desertification of western South America. Geology 30, 43–46.

Hayakawa, Y.S., Oguchi, T., Lin, Z., 2008. Comparison of new and existing global digital elevation models: ASTER G-DEM and SRTM-3. Geophysical Research Letters 35, L17404. doi:10.1029/2008GL035036.

Hayashi, S., Kamata, K., Ban, M., Umeda, K., 1999. Erosion rate of stratovolcanoes — a case study of northeast Japan. Japan Geoscience Union Meeting, Abstract, VC-013.

Hirt, C., Filmer, M.S., Featherstone, W.E., 2010. Comparison and validation of recent freely-available ASTER-GDEM ver1, SRTM ver4.1 and GEODATA DEM-9S ver3 digital elevation models over Australia. Australian Journal of Earth Sciences 57 (3), 337–347. doi:10.1080/08120091003677553.

Hoke, G.D., Garzione, C.N., 2008. Paleosurfaces, paleoelevation, and the mechanisms for the latest Miocene topographic development of the Altiplano Plateau. Earth and Planetary Science Letters 271 (1–4), 192–201. doi:10.1016/j.epsl.2008.04.008.

Hora, J.M., Singer, B.S., Wörner, G., 2007. Eruptive flux during periods of cone growth and collapse at Volcan Parinacota, Chilean CVZ, from a high-resolution $^{40}Ar/^{39}Ar$ eruptive chronology. Geological Society of America Bulletin 119 (3/4), 343–362.

Horton, B.K., 1999. Erosional control on the geometry and kinematics of thrust belt development in the central Andes. Tectonics 18 (6), 292–1293.

Huggel, C., Schneider, D., Julio Miranda, P., Delgado Granados, H., Kääb, A., 2008. Evaluation of ASTER and SRTM DEM data for lahar modeling: a case study on lahars from Popocatépetl Volcano, Mexico. Journal of Volcanology and Geothermal Research 170, 99–110. doi:10.1016/j.jvolgeores.2007.09.005.

Isacks, B.L., 1988. Uplift of the Central Andean Plateau and bending of the Bolivian Orocline. Journal of Geophysical Research 93 (84), 3211–3231.

Kaneoka, I., Guevara, C., 1984. K–Ar age determinations of late Tertiary and Quaternary Andean volcanic rocks, southern Peru. Geochemical Journal 18, 233–239.

Karátson, D., 1996. Rates and factors of stratovolcano degradation in a continental climate: a complex morphometric analysis of nineteen Neogene/Quaternary crater remnants in the Carpathians. Journal of Volcanology and Geothermal Research 73, 65–78.

Karátson, D., Timár, G., 2005. Comparative volumetric calculations of two segments of the Carpathian Neogene/Quaternary volcanic chain using SRTM elevation data: implications to erosion and magma output rates. Zeitschrift fur Geomorphologie Supplementband 140, 19–35.

Karátson, D., Favalli, M., Tarquini, S., Fornaciai, A., Wörner, G., 2010a. The regular shape of stratovolcanoes: a DEM-based morphometrical approach. Journal of Volcanology and Geothermal Research 193, 171–181.

Karátson, D., Telbisz, T., Singer, B., 2010b. Late-stage volcano geomorphic evolution of the Pleistocene San Francisco Mountain, Arizona (USA), based on high-resolution DEM analysis and $^{40}Ar/^{39}Ar$ chronology. Bulletin of Volcanology 72, 833–846.

Kervyn, M., Ernst, G.G.J., Goossens, R., Jacobs, P., 2008. Mapping volcano topography with remote sensing: ASTER vs SRTM. International Journal of Remote Sensing 29, 6515–6538. doi:10.1080/01431160802167949.

Klein, A.G., Seltzer, G.O., Isacks, B.L., 1999. Modern and last glacial maximum snowlines in the Peruvian–Bolivian Andes. Quaternary Science Reviews 18, 63–84.

Klemetti, E.W., Grunder, A.L., 2008. Volcanic evolution of Volcán Aucanquilcha: a long-lived dacite volcano in the Central Andes of northern Chile. Bulletin of Volcanology 70, 633–650.

Kober, S., Ivy-Ochs, S., Schlunegger, F., Baur, H., Kubik, P.W., Wieler, R., 2007. Denudation rates and a topography-driven rainfall threshold in northern Chile: multiple cosmogenic nuclide data and sediment yield budgets. Geomorphology 83 (1–2), 97–120.

Lamb, S., Davis, P., 2003. Cenozoic climate change as a possible cause for the rise of the Andes. Nature 425 (23, October).

MacDonald, G.A., 1972. Volcanoes. Prentice-Hall, Inc, Englewood Cliffs, New Jersey. (510 pp.).

Mamani, M., Wörner, G., Sempere, T., 2010. Geochemical variations in igneous rocks of the Central Andean Orocline. Geological Society of America Bulletin 122, 162–182.

Matteini, M., Mazzuoli, R., Omarini, R., Cas, R., Maas, R., 2002. Geodynamical evolution of the Central Andes at ^{24}Os as inferred by magma composition along the Calama–Olacapato–El Toro transversal volcanic belt. Journal of Volcanology and Geothermal Research 118, 205–228.

McKee, E.H., Robinson, A.C., Rybuta, J.J., Cuitino, L., Moscoso, R.D., 1994. Age and Sr isotopic composition of volcanic rocks in the Maricunga Belt, Chile: implications for magma sources. Journal of South American Earth Sciences 7 (2), 167–177.

Mortimer, C., Farrar, E., Saric, N., 1974. K–Ar ages from Tertiary lavas of the northernmost Chilean Andes. Geologische Rundschau 63, 484–493.

Ollier, C.D., 1988. Volcanoes. Basil Blackwell, Oxford. (228 pp.).

Placzek, C.J., Quade, J., Patchett, P.J., 2006. Geochronology and stratigraphy of late Pleistocene lake cycles on the southern Bolivian Altiplano: implications for causes of tropical climate change. Geological Society of America Bulletin 118, 515–532.

Placzek, C.J., Matmon, A., Granger, D.E., Quade, J., Niedermann, S., 2010. Evidence for active landscape evolution in the hyperarid Atacama from multiple terrestrial cosmogenic nuclides. Earth and Planetary Science Letters 295, 12–20.

Rabus, B., Eineder, M., Roth, A., Bamler, R., 2003. The shuttle radar topography mission — a new class of digital elevation models acquired by spaceborne radar. Journal of Photogrammetry and Remote Sensing 57, 241–262.

Riquelme, R., Darrozes, J., Maire, E., Hérail, G., Soula, J.C., 2008. Long-term denudation rates from the Central Andes (Chile) estimated from a Digital Elevation Model using the Black Top Hat function and Inverse Distance Weighting: implications for the Neogene climate of the Atacama Desert. Revista Geologica de Chile 35 (1), 105–121.

Rodriguez, E., Morris, C.S., Belz, J.E., Chapin, E.C., Martin, J.M., Daffer, W., Hensley, S., 2005. An Assessment of the SRTM Topographic Products. JPL Pub. (D31639, 143 pp.).

Please cite this article as: Karátson, D., et al., Erosion rates and erosion patterns of Neogene to Quaternary stratovolcanoes in the Western Cordillera of the Central Andes: An SRTM DEM based analysis, Geomorphology (2011), doi:10.1016/j.geomorph.2011.10.010

Ruxton, B.P., McDougall, I., 1967. Denudation rates in Northeast Papua from potassium–argon datings of lavas. American Journal of Science 265, 545–561.
Schildgen, T.F., Hodges, K.V., Whipple, K.X., Reiners, P.W., Pringle, M.S., 2007. Uplift of the western margin of the Andean plateau revealed from canyon incision history, southern Peru. Geology 35 (6), 523–526.
Schildgen, T.F., Ehlers, T.A., Whipp Jr., D.M., vanSoest, M.C., Whipple, K.X., Hodges, K.V., 2009a. Quantifying canyon incision and Andean Plateau surface uplift, southwest Peru: a thermochronometer and numerical modeling approach. Journal of Geophysical Research, Earth Surface 114, F04014. doi:10.1029/2009JF001305.
Schildgen, T.F., Hodges, K.V., Whipple, K.X., Pringle, M.S., vanSoest, M., Cornell, K.M., 2009b. Late Cenozoic structural and tectonic development of the western margin of the Central Andean Plateau in southwest Peru. Tectonics 28, TC4007. doi:10.1029/2008TC002403.
Schildgen, T.F., Balco, G., Shuster, D.L., 2010. Canyon incision and knickpoint propagation recorded by apatite $He/^{3}He$ thermochronometry. Earth and Planetary Science Letters 293, 377–387.
Stern, C.A., 2004. Active Andean volcanism: its geologic and tectonic setting. Revista Geologica de Chile 31 (2), 161–206.
Strasser, M., Schlunegger, F., 2005. Erosional processes, topographic length-scales and geomorphic evolution in arid climatic environments: the 'Lluta collapse', northern Chile. International Journal of Earth Sciences (Geologische Rundschau) 94, 433–446.
Strecker, M.R., Alonso, R., Bookhagen, B., Carrapa, B., Hilley, G.E., Sobel, E.R., Trauth, M.H., 2007. Tectonics and climate of the Southern Central Andes. Annual Review of Earth and Planetary Sciences 35, 747–787. doi:10.1146/annurev.earth.35.031306.140158.
Summerfield, M.A., 1991. Global geomorphology. An Introduction to the Study of Landforms. Longman Sci. Tech., Harlow, copublished with Wiley, New York, NY (537 pp.).
Thouret, J.C., Finizola, A., Fornari, M., Legeley-Padovani, A., Suni, J., Frechen, M., 2001. Geology of El Misti volcano near the city of Arequipa, Peru. GSA Bulletin 113 (12), 1593–1610.
Thouret, J.C., Wörner, G., Singer, B., Gunnell, Y., Zhang, X., Souriot, T., 2007. Landscape evolution on the western Andean slope in southern Peru: incision of deepest Andean canyons during Miocene uplift of the Central Andes. Earth and Planetary Science Letters 263, 151–166.
Trumbull, R.B., Riller, U., Scheuber, E., Hongn, F., 2006. The time-space distribution of Cenozoic arc volcanism in the Central Andes: a new data compilation and its tectonic implications. In: Oncken, O., Chong, G., Franz, G., Giese, P., Götze, H.J., Ramos, V.A. (Eds.), The Andes — active subduction orogeny: Frontiers in Earth Sciences, vol. 1. Springer, pp. 29–43.
Vandervoort, D.S., Jordan, T.E., Zeitler, P.K., Alonso, R.N., 1995. Chronology of internal drainage development and uplift, southern Puna plateau, Argentine central Andes. Geology 23 (2), 145–148.
Willenbring, J.K., von Blanckenburg, F., 2010. Long-term stability of global erosion rates and weathering during late-Cenozoic cooling. Nature 465, 211–214.
Wood, C.A., 1978. Morphometric evolution of composite volcanoes. Geophysical Research Letters 5/6, 437–439.
Wörner, G., Harmon, R.S., Davidson, J., Moorbath, S., Turner, D.L., Mcmillan, N., Nye, C., Lopez-Escobar, L., Moreno, H., 1988. The Nevados de Payachata volcanic region (18°S/69°W, N. Chile): I. Geological, geochemical, and isotopic observations. Bulletin of Volcanology 50 (5), 287–303. doi:10.1007/BF01073587.
Wörner, G., Hammerschmidt, K., Henjes-Kunst, F., Lezaun, J., Wilke, H., 2000. Geochronology ($^{40}Ar/^{39}Ar$, K/Ar and He-exposure ages) of Cenozoic magmatic rocks from northern Chile (18′22°S): implications for magmatism and tectonic evolution of the central Andes. Revista Geologica de Chile 27 (2), 205–240.
Wörner, G., Uhlig, D., Kohler, I., Seyfried, H., 2002. Evolution of the West Andean Escarpment at 18°S (N. Chile) during the last 25 Ma: uplift, erosion and collapse through time. Tectonophysics 345, 183–198.
Wright, R., Garbeil, H., Baloga, S.M., Mouginis-Mark, P.J., 2006. An assessment of shuttle radar topography mission digital elevation data for studies of volcano morphology. Remote Sensing of Environment 105, 41–53. doi:10.1016/j.rse.2006.06.002.

Please cite this article as: Karátson, D., et al., Erosion rates and erosion patterns of Neogene to Quaternary stratovolcanoes in the Western Cordillera of the Central Andes: An SRTM DEM based analysis, Geomorphology (2011), doi:10.1016/j.geomorph.2011.10.010